

Heavy-Ion Collisions - Examining the Quark Gluon Plasma at RHIC

Helen Caines,¹

(1) *Physics Department, Yale University, New Haven, CT 06520, U.S.A*

Abstract

The main goals of relativistic heavy-ion experiments is to study the properties of QCD matter under extreme temperatures and densities. The focus of this talk is the studies that are underway at the Relativistic Heavy Ion Collider (RHIC), located at the Brookhaven National Laboratory (BNL) on Long Island, New York, U.S.A. I discuss selected highlights from the past couple of years that are key to elucidating the characteristics of the new state of matter created in these heavy-ion collisions, called a Quark Gluon Plasma.

1. Introduction

The goals of the experiments at the Relativistic Heavy Ion Collider (RHIC) are to study hot QCD matter, and investigate the spin structure of the proton. RHIC has now been running for nearly a decade, and has collided a diverse set of beams from p to Au ions at $\sqrt{s_{NN}} = 20\text{-}200$ GeV (p beams have just been collided at $\sqrt{s} = 500$ GeV). Initially there were four RHIC experiments BRAHMS [1], PHENIX [2], PHOBOS [3], and STAR [4]. Only the two large multi-purpose experiments, PHENIX and STAR, remain in operation, BRAHMS and PHOBOS completed their programs and have been de-commissioned. This talk focuses on recent results from these two collaborations, which highlight our progress in probing the properties of the new state of matter, called a Quark Gluon Plasma (QGP), created in relativistic heavy-ion collisions.

At sufficiently high temperatures it has long been predicted that strongly interacting matter, described by QCD, must “melt” into a deconfined phase of quarks and gluons [5]. Lattice calculations indicate that at non-zero baryo-chemical potential the critical temperature for such a transition is $T_C 150\text{-}180$ MeV [6]. There is clear evidence for the RHIC experiments that such a deconfined phase, the QGP, is created in Au-Au collisions at $\sqrt{s_{NN}} = 200$ GeV. The initial energy density in the collision region is greater than 4.6 GeV/fm⁴ [7] and the initial temperature is $T=300\text{-}600$ MeV [8], which are much higher than that where hadrons can exist. The degrees of freedom in the initial stages are those of quarks and gluons. Together these results show that a new partonic state of matter exists in the early stages of these heavy-ion collisions and that this matter flows like an almost “perfect” liquid [9, 10, 11, 12]. An initially surprising result was that the medium is almost opaque to color charges passing through it. In deference to this discovery the plasma is now frequently referred to as the “sQGP”, or strongly coupled QGP. The use of high transverse momentum probes (jets) to elucidate the properties of the sQGP are the topic of the first section of my talk. The second section discusses the tantalizing suggestion of observation of local strong parity violation in heavy-ion collisions where partonic degrees of freedom exist. Finally, I briefly discuss two exciting new avenues in relativistic heavy-ion studies that will become available in the next couple of years.

2. Jets as Probes of the sQGP

At RHIC energies high transverse momentum (p_T), or Q^2 , scatterings can only occur in the initial parton-

parton interactions. This means that a) the integrated yield of hard processes must scale with the number of binary nucleon-nucleon interactions in the collisions (binary scaling) and b) in heavy-ion events the scattered partons must pass through the matter produced before they escape the medium and fragment. Hence, we have a direct, and calibrated, probe of the partonic phase of the collision. These interactions with the medium will result in the attenuation and/or complete absorption of the energy of the jet into the bulk. By comparing the measured jet rates and properties, as a function of p_T , with those from p-p events at the same collision energy we can extract details about the sQGP's properties.

2.1. Di-hadron Correlations

Measuring jets in the heavy-ion environment is a highly non-trivial task. First studies utilized high p_T leading particle as proxies for full jet reconstruction and di-hadron correlations. A high p_T “trigger” particle is selected and the $\Delta\phi$ distribution of all other associated particles in the events constructed. In p-p collisions clear jet peaks are observed at $\Delta\phi=0$ and π , (solid histogram in Fig. 1.). However, while a clear peak is seen at $\Delta\phi=0$ in the central Au-Au data (blue stars), it has disappeared on the away side ($\Delta\phi=\pi$). The presence of the away side peak in the d-Au data (red circles), where no QGP is created, shows that this jet quenching phenomena is not caused by initial or final state cold matter effects [13]. The quenching of the away-side jet in Au-Au collisions must therefore be due to interactions of the partons with the sQGP. In addition, the high p_T particle yields in central Au-Au collisions have been shown to be suppressed by a factor of five compared to binary scaled p-p yields [14].

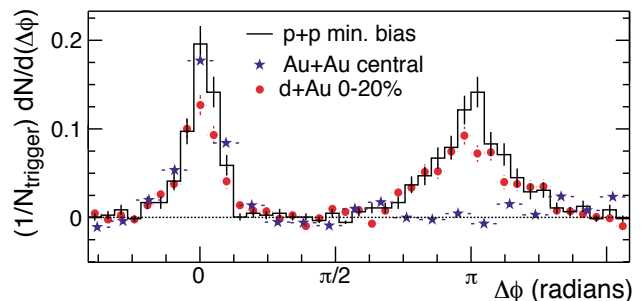


Fig. 1. Color Online: Di-hadron $\Delta\phi$ correlations for p-p (solid histogram), 0-20% d-Au (red circles) and central Au-Au (blue stars) collisions at $\sqrt{s_{NN}} = 200$ GeV. Figure from [13].

The suppression of single high p_T particles and the quenching of the away-side jet are both interpreted as dominantly due to multiple final-state gluon radiation off the hard scattered partons, that is induced by the presence of the dense colored medium (the sQGP). The magnitude of the partonic energy loss depends on the length of the medium traversed and the transport coefficient \hat{q} , which is the mean squared p_T transferred per unit length [15]. Current data constrain model-dependent

calculations of $\langle \hat{q} \rangle$ to within $\pm 20\text{-}30\%$ [16]. However the theoretical uncertainties are still large and estimates of $\langle \hat{q} \rangle$ range from 5-15 GeV²/fm.

Although much has been learned by studying single particle high p_T yields and di-hadron correlations, exact connections to pQCD calculations were limited since they are only indirect measurements of jets. In principle, only by direct jet reconstruction can the initial parton energy be fully recovered.

2.2. Jet reconstruction

The high multiplicity created in heavy-ion events means that all jets are sat on a large, and fluctuating background. However, as shown in Fig. 2, a jet of ~ 20 GeV is still clearly visible above the background when the charged and neutral energy is taken into account, meaning that while the background cannot be ignored, jet reconstruction in Au-Au events is possible.

The two RHIC experiments currently utilize different jet finders. STAR uses a set of three different algorithms from the FastJet package [17], the seedless cone algorithm (SIScone), and the k_T and Anti- k_T recombination codes. PHENIX meanwhile use a seedless Gaussian filter [18, 19]. All of these jet finders are infrared and collinear safe. Both experiments use charged tracking detectors and electro-magnetic calorimetry at mid-rapidity to perform their studies

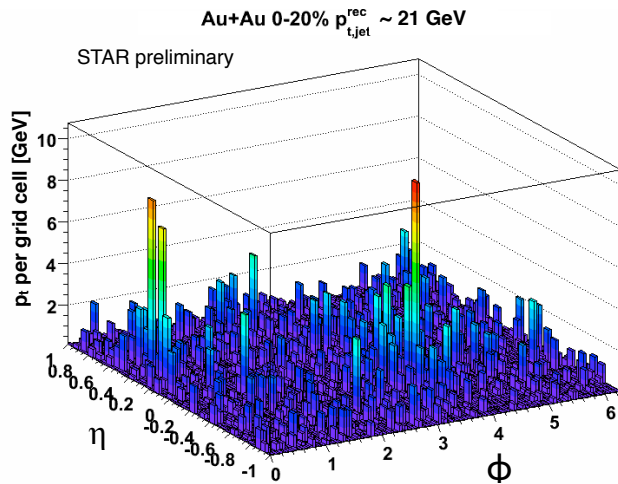


Fig. 2. Color Online: The summed neutral and charged p_T in a 0-20% central Au-Au collisions at $\sqrt{s_{NN}} = 200$ GeV in $\eta - \phi$ space for an event with a reconstructed di-jet of $p_T^{rec} \approx 20$ GeV/c. Figure from [20].

Before the Au-Au analyses could proceed it was necessary to ensure that jet production in p-p collisions at RHIC is a calibrated probe that is well described by pQCD calculations. We find that the inclusive jet cross-section agrees with NLO predictions over seven orders of magnitude [21]. The charged particle fragmentation functions have been extracted and are shown in Fig. 3. for reconstructed jet p_T of 20-30 GeV/c and resolution parameters of $R=0.4$ and 0.7. Charged particles with $p_T > 0.2$ GeV/c and calorimeter towers with $E_T > 0.2$ GeV are included in the study. These data have not yet been corrected to the particle level, therefore the results are compared to PYTHIA 6.410, Tune A [22, 23]. These calculations passed through STAR's detector simulation and reconstruction algorithms. The single charged particle reconstruction efficiency in the TPC is $> 80\%$ for $p_T > 1$ GeV/c, but drops steeply for lower p_T . Such de-

tor inefficiencies and the presence of particles which are undetected by the STAR detector, such as the neutron and K_L^0 , cause the reconstructed jet p_T to be lower on average than the true value. Good agreement is seen between PYTHIA and the data for jet algorithm resolution parameters $R=0.4$ and 0.7 suggesting that there are no significant large angle initial/final state radiation effects beyond those accounted for by this LO calculation. Data from studies of the underlying event in p-p events by STAR also support this conclusion [24].

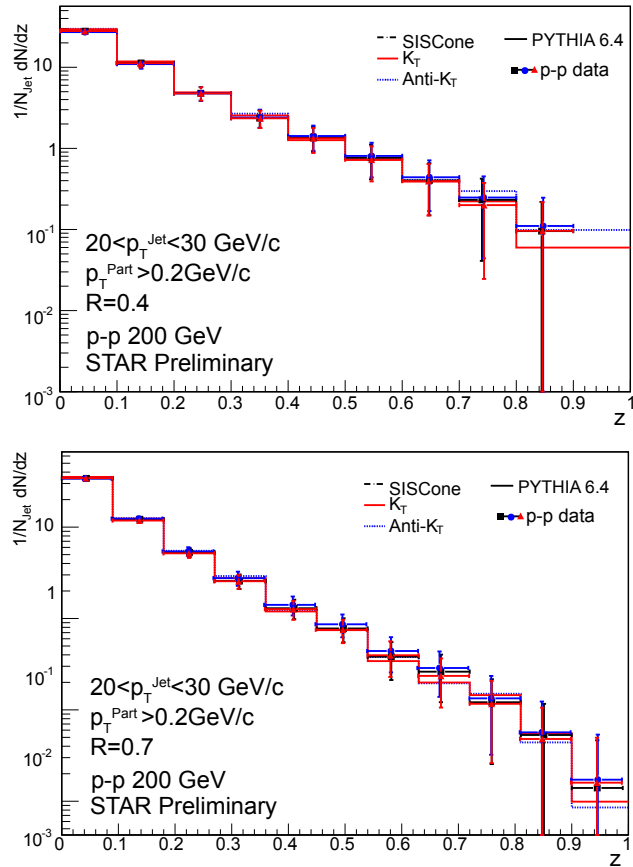


Fig. 3. Color online: Charged particle, detector level, z fragmentation functions for jets reconstructed with $20 < p_T < 30$ GeV/c in $\sqrt{s} = 200$ GeV p-p collisions, compared to PYTHIA for 3 different jet algorithms. $|\eta| < 1-R$, for $R=0.4$ (top) and $R=0.7$ (bottom). Red triangles - k_T , blue circles - Anti- k_T and SIScone - black squares. The errors are statistical only. Figure from [25].

Once again initial state effects on jet properties need to be disentangled from those of the medium. Di-hadron correlations showed that the away-side signal was not suppressed in d-Au collisions but the affect of nuclear k_T remained to be determined. The intrinsic k_T of the nucleons in the nuclei and the additional scattering of the parton in matter before fragmentation results in the scattered parton pairs no longer being exactly back-to-back in $\Delta\phi$. This effect can be measured as a broadening of the $\Delta\phi$ di-jet correlation in d-Au compared to p-p collisions. We therefore measure $k_{T,raw} = p_{T,1} \sin(\Delta\phi)$, where $p_{T,1}$ is the highest jet p_T of the di-jet pair and $\Delta\phi$ is the angle between the jets. Figure 4. shows the measured $k_{T,raw}$ distributions from p-p collisions in the left plot and d-Au collisions in the right plot for 10 GeV/c $< p_{T,2} < 20$ GeV/c. The extracted $\sigma_{k_{T,raw}}^{p-p} = 2.8 \pm$

0.1 (stat) GeV/c and $\sigma_{k_T,raw}^{d-Au} = 3.0 \pm 0.1$ (stat) GeV/c from Gaussian fits to the data indicate that any additional broadening due to nuclear effects is small.

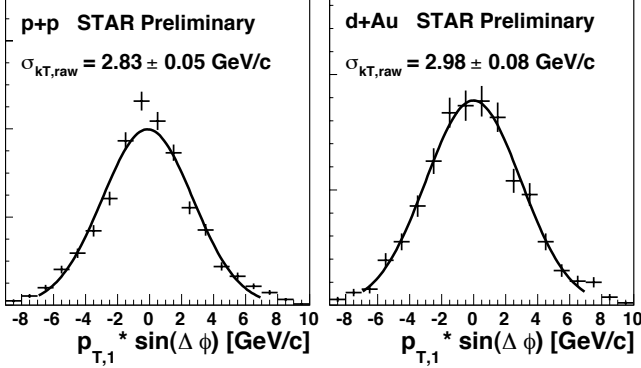


Fig. 4. Color online: Measured $k_{T,raw}$ distributions from p-p collisions (left) and d-Au (right) $\sqrt{s_{NN}} = 200$ GeV collisions for $10 \text{ GeV}/c < p_{T,2} < 20 \text{ GeV}/c$. The solid curves are Gaussian fits to the data. Figure from [26].

Much work has been invested in developing codes and techniques that will allow us to extract jets from the underlying event background in heavy-ion collisions. These techniques avoid, as far as possible, a reliance on theoretical assumptions as to the modification of the jet structure in Au-Au due to the interactions with the medium. First we needed to estimate the energy per unit area, ρ , of the background and its region-to-region fluctuations, σ , in a given event. Schematically, the reconstructed jet $p_T \sim p_T^{jet} + \rho A \pm \sigma \sqrt{A}$, where A is the jet cone area. In a central Au-Au event $\rho \sim 45 \text{ GeV}$ for $R=0.4$ and $\sigma \sim 6-7 \text{ GeV}$ when a p_T cut of $0.2 \text{ GeV}/c$ is applied to all particles in the event. The scale of the fluctuations can be significantly suppressed by increasing the p_T cut or decreasing the jet cone radius (resolution parameter), but only at the expense of the jet energy resolution and the loss of information about the softest part of the fragmentation [27].

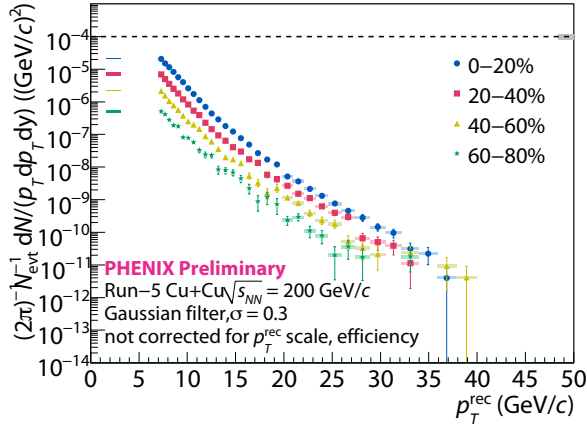


Fig. 5. Color online: Fake rejected raw jet spectrum for Cu+Cu $\sqrt{s_{NN}} = 200$ GeV collisions using $\sigma = 0.3$ Gaussian filter, $g\sigma_{dis} > 17.8 (\text{GeV}/c)^2$ fake rejection. Figure from [28].

Figures 5. and 6. show the inclusive jet cross-sections for various centralities in Cu-Cu collisions [28] and 0-10% central Au-Au collisions [29] at $\sqrt{s_{NN}} =$

200 GeV respectively. These results, and those presented in [20], represent the first time that jets have been reconstructed in heavy-ion collisions and constitute a giant leap forward in RHIC physics. Figure 5. is the raw reconstructed Cu+Cu jet spectrum for different centralities using a $\sigma = 0.3$ Gaussian filter. In this analysis fake jets are rejected by ensuring that $g\sigma_{dis}(\eta, \phi) = \sum_{i \in \text{fragment}} p_{T,i}^2 e^{-((\eta_i - \eta)^2 + (\phi_i - \phi)^2)/2\sigma_{dis}} > 17.8 (\text{GeV}/c)^2$, $\sigma_{dis} = 0.1$. Fake jets are defined as the random clustering of energy that does not come from the fragmentation of a hard scattered parton into a “jet” candidate. A consistent power-law shape across all centralities is evident.

In Fig. 6. the k_T and Anti- k_T jet finding algorithms are used. To obtain the Au-Au inclusive jet yields the raw spectra are corrected for fake jets, tracking inefficiencies, and the missed neutral energy, including K_L^0 and neutrons. The spectra are also unfolded to account for jet energy resolution and background fluctuations.

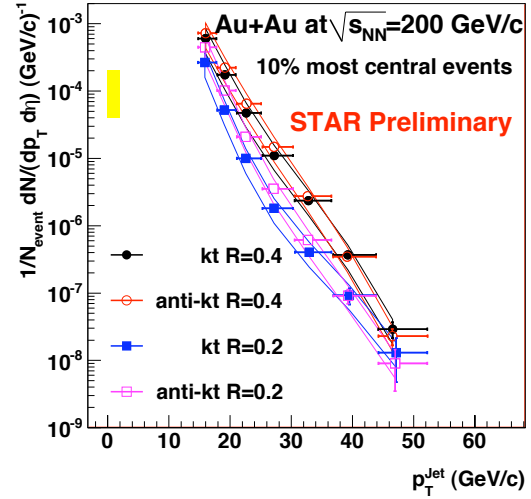


Fig. 6. Color online: Cross sections for inclusive jet production in Au + Au collisions at $\sqrt{s_{NN}} = 200$ GeV (k_T and Anti- k_T , $R = 0.2$ and 0.4) $|\eta| < 1-R$. The systematic uncertainty on the jet energy scale, shown as the vertical shaded band, is dominated by the uncertainties on the electro-magnetic calorimeter calibration (5%), unobserved jet energy (3%), and charged component momentum resolution (2%). Solid curves represent the systematic uncertainty on the jet yield in Au+Au due to background fluctuations. Figure from [29].

The quenching effects of the medium discussed above will cause jet fragmentation functions in A-A collisions to be highly modified. The emitted gluon radiation results in numerous soft particles being produced enhancing the yield of low z particles. At the same time there will be a corresponding suppression of high z fragments. However, energy and momentum must be conserved even in the presence of jet quenching. Therefore if we can perform unbiased jet reconstruction the total initial partonic energy must be recovered, albeit with a re-distribution of the internal jet structure. The nuclear modification factor is defined as:

$$R_{AA} = \frac{Yield(A - A)}{Yield(p - p) \langle N_{coll} \rangle} \quad (1)$$

where $\langle N_{coll} \rangle$ is the average number of binary nucleon-nucleon collisions in the A-A collision, estimated via a

Glauber calculation [30]. If the jet reconstruction is unbiased then $R_{AA} = 1$, if not all the energy is recovered then $R_{AA} < 1$. Figure 7. shows the nuclear modification factor for jets in 0-10% Au-Au collisions for $R=0.4$ and 0.2 using the k_T and Anti- k_T jet algorithms. It can be seen that the R_{AA} for $R=0.4$ is compatible with unity, within the large uncertainties. The R_{AA} for $R=0.2$ for reconstructed $p_T^{jet} > 20$ GeV/c on the other hand is markedly lower. There are significant differences between the results for the k_T and Anti- k_T algorithms. This is under investigation, but most likely arises from their different responses to the heavy-ion background [17].

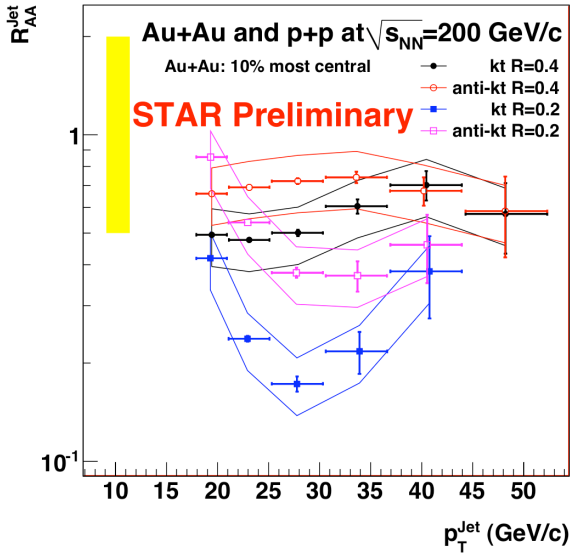


Fig. 7. Color online: Jet R_{AA} for $\sqrt{s_{NN}} = 200$ GeV 0-10% Au-Au collisions for k_T and Anti- k_T , $R = 0.2$ and 0.4 . Figure from [29].

Figure 8. shows the ratio of inclusive jet cross-section for $R=0.2/R=0.4$ jet resolution parameters for p-p and Au-Au data. This ratio increases with reconstructed jet energy for p-p collisions, as expected, due to the focussing of the jet fragmentation with increasing partonic energy. However, the Au-Au data shows a different trend, the ratio is approximately flat. In this representation, there is no difference in the results from the k_T and Anti- k_T jet algorithms, supporting the notion that the differing results observed in Fig. 7. are indeed due to their behaviors in the presence of the large background in Au-Au events.

2.3. Jet-hadron Correlations

Figure 7. and 8. indicate that the presence of the medium results in a sizeable de-focussing of the jet resulting in significant amounts of the initial partonic energy being lost. To study this further we use jet-hadron correlations. First the Anti- k_T algorithm with a resolution parameter of $R=0.4$ is run on events where only charged tracks and electromagnetic calorimeter towers with $p_T > 2$ GeV/c are considered. If a jet is reconstructed with $p_T > 20$ GeV/c the $\Delta\phi$ of charged particles is calculated with respect to the jet axis. This jet-hadron correlation allows the study of the away-side jet even in the case that this di-jet partner would not be

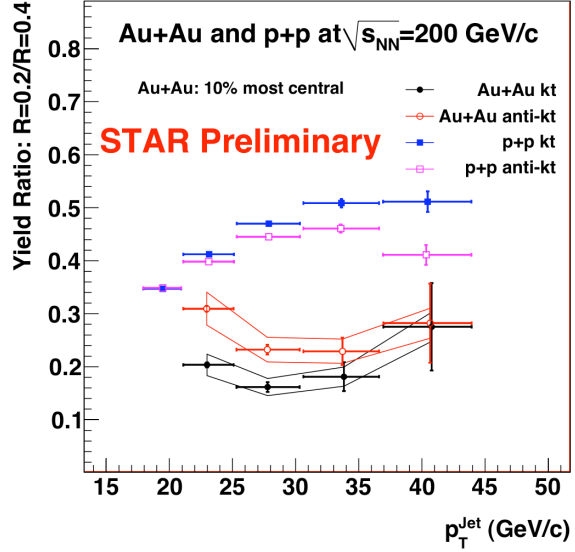


Fig. 8. Color online: Ratios of the $R=0.2/R=0.4$ inclusive jet cross sections for $\sqrt{s_{NN}} = 200$ GeV p-p and 0-10% Au-Au collisions using k_T and Anti- k_T algorithms. Figure from [29].

reconstructed via standard jet algorithms. The resulting correlations are shown in Fig. 9. for associated hadrons with $0.2 < p_T < 1.0$ GeV/c (left panel) and $p_T > 2.5$ GeV/c (right panel). It can be seen (right panel) that for high p_T associated particles the away side jet is dramatically suppressed in Au-Au compared to p-p collisions. However, for the low p_T associated particles the Au-Au data is not only strongly enhanced but also significantly broader, with significant enhancement beyond a radius of 0.4 . Using this type of analysis will allow us to establish the scale of the “out-of-cone” radiation emitted by the parton, which is not possible with conventional jet reconstruction. This result represents the first direct measurement of the “modified fragmentation” of jets in the presence of the sQGP.

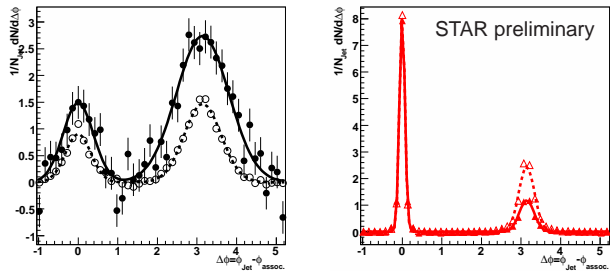


Fig. 9. Color online: Jet-hadron $\Delta\phi$ correlations. Reconstructed jet $p_T > 20$ GeV/c, using Anti- k_T algorithm, $R=0.4$ and $p_T > 2$ GeV/c for all charged particles and towers. Left: Associated particles $0.2 < p_T < 1.0$ GeV/c and Right: Associated particles $p_T > 2.5$ GeV/c. The open symbols are for p-p collisions and the closed symbols for 0-10% Au-Au $\sqrt{s_{NN}} = 200$ GeV collisions. Figure from [31].

2.4. Summary of Jet Studies

Jet studies are well under way at RHIC. The p-p reference measurements are well described by theoretical calculations, indicating that we have a calibrated probe to turn on the heavy-ion medium. The underlying event in p-p collisions is small and the measurements indicate that there is little to no large angle initial and final state radiation. In addition the cold nuclear matter effects, as measured via d-Au collisions, are minimal.

The background due to the hadronization of the sQGP created at RHIC, while significant, can be statistically subtracted from the reconstructed jets. There is strong evidence that the partons resulting from initial high Q^2 scatterings lose significant energy as they traverse the colored medium. Their jet profile is strikingly broadened and the hadrons produced have much softer p_T on average than jets fragmenting in vacuum, as determined via p-p collisions at the same beam energy.

3. Local Strong Parity Violation

Although parity violation in weak interactions was first observed in 1975 [32], until recently it was thought to be conserved in strong interactions. Modern QCD calculations now allow for such parity violation but to date it has not been observed. It has been suggested that in relativistic heavy-ion collisions parity-odd domains may be created which correspond to non-trivial topological solutions of the QCD vacuum thus violating parity and time-reversal symmetries locally [33]. In non-central collisions, significant orbital angular momentum and an extremely large magnetic field, albeit short lived, are created when the two nuclei collide. The non-zero topological charge domains produce different numbers of positive and negative quarks in each domain. The interaction of these particles with the strong B-field results in a charge separation of quarks along the systems orbital momentum axis [34, 35, 36]. A clear division of charge along the angular momentum vector would therefore be evidence of local strong parity violation.

In any given event this charge separation along the angular momentum vector may be described by

$$\frac{dN_{\pm}}{d\phi} \approx (1 + 2v_1 \cos(\Delta\phi) + 2v_2 \cos(2\Delta\phi) + \dots + 2a_{\pm} \sin(\Delta\phi) + \dots),$$

where $\Delta\phi$ is the azimuthal angular difference of each particle with respect to the reaction plane. The reaction plane is defined by the beam axis and the line joining the centers of the two colliding nuclei. v_1 and v_2 etc are the coefficients that account for the so-called directed and elliptic flow [37]. The “ a ” parameters, where $a_+ = -a_-$, measure the parity violating effect. However, since this is a spontaneous effect the sign of a_+ (and hence a_-) is random in each event, when averaged over many events this parity odd observable therefore yields, $\langle a_+ \rangle = \langle a_- \rangle = 0$.

It was therefore suggested [38] to instead detect

$$\langle a_{\alpha} a_{\beta} \rangle \approx \langle \cos(\phi_{\alpha} + \phi_{\beta} - 2\Psi_{RP}) \rangle$$

where α and β are the sign of the electric charge of the particles sampled and Ψ_{RP} is the reaction plane angle. Experimentally this can be measured via a three particle correlation since

$$\langle \cos(\phi_{\alpha} + \phi_{\beta} - 2\Psi_{RP}) \rangle = \langle \cos(\phi_{\alpha} + \phi_{\beta} - 2\phi_c) \rangle / v_{2,c}$$

where the three particles are labelled α, β , and c . It is assumed that the only common correlation between

particles α, β and c is via the reaction plane, and particle c is used only to determine the angle of the event plane.

Assuming this correlation to be only sensitive to the parity violation effect, and ignoring any final state interactions with the medium, then $\langle a_+ a_+ \rangle = \langle a_- a_- \rangle = -\langle a_+ a_- \rangle > 0$. This correlator should also scale inversely with the number of particles produced, assuming the domain sizes stay constant. However, it seems extremely likely that there are interactions with the medium the predicted effect of these interactions is a suppression of the back-to-back 3 particle correlation (one of the charged pairs has to make its way through the medium) resulting in $\langle a_+ a_+ \rangle = \langle a_- a_- \rangle >> \langle a_+ a_- \rangle$.

Figure 10. shows the correlations for Au-Au collisions at $\sqrt{s_{NN}} = 200$ GeV as a function of centrality for same-sign and opposite-sign charge values of α and β . As expected for the parity violation signal, the absolute magnitude of the opposite-charge correlations are smaller than the same-charge correlations, and the sign of the correlations are opposite. The predicted inverse dependence on centrality is observed.

However, since this measure is now parity-even it is possible for other effects to produce a non-zero signal. Examples of such physics backgrounds considered are coulomb effects, the decay of resonances, jet fragmentation and collective motion of the bulk. One technique used to investigate such possibilities was the calculation of the three particle correlation described above for the HIJING [39], UrQMD [40] and MeVSim [41] heavy-ion event generators. The results are also shown in Fig. 10. MeVSim only includes correlations due to resonance decays and overall elliptic flow, while HIJING and UrQMD are real physics models of the collisions and therefore include correlations due to many physical processes. It can be seen that none of these generators can reproduce the data. So far no non-parity violating signals have been found, via our systematic checks, that can explain the magnitude, sign and centrality dependence of both the like- and opposite-sign correlations. For further details of these studies see [42].

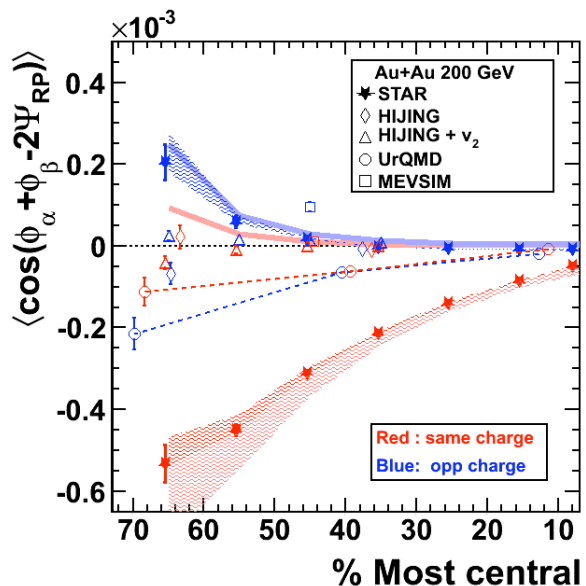


Fig. 10. Color Online: $\langle \cos(\phi_{\alpha} + \phi_{\beta} - 2\Psi_{RP}) \rangle$ calculated from data from Au+Au collisions at $\sqrt{s_{NN}} = 200$ GeV collisions by the STAR experiment. Also shown are the same calculations from the HIJING (with and without elliptic flow “after burners”), UrQMD, and MeVSim event generators. From [44].

4. The Next Frontiers

Current relativistic heavy-ion experiments are poised to explore two exciting new frontiers: 1) the new energy regime made accessible with the turn-on of the Large Hadron Collider (LHC), scheduled for November 2009 and 2) a Beam Energy Scan at RHIC set to start in 2010.

4.1. Beam Energy Scan

Theory calculations can be used to predict how transitions to a sQGP depend on the baryon chemical potential, μ_B , and temperature, T . At low μ_B and high T a cross-over transition is predicted, while at high μ_B and low T the transition is of first order. Hence, at intermediate values, a critical point should occur (see for example [43]). Experimentally we can vary these initial conditions by altering the beam energy. At RHIC we can explore the range from $\sqrt{s_{NN}} = 5$ -200 GeV covering the μ_B range of 500-20 MeV. The phase diagram of nuclear matter is depicted in Fig. 11. The yellow curves in the figure are the trajectories expected for the various collision energies selected for the beam energy scan (BES). After thermalization, the system rapidly cools and expands before passing through the phase transition from the sQGP to a hadronic gas. Inelastic hadronic re-scatterings continue until chemical freeze-out is reached, at which point the ratio of particle species is locked in. Elastic interactions continue until the system passes through kinetic freeze-out, at which point the hadrons free stream to the detectors. Theoretical calculations are not currently able to determine the exact location of the critical point. It has therefore been suggestively placed in the centre of the range of the RHIC BES. A RHIC beam energy scan will allow us to explore the QCD phase diagram close to the QGP-hadron gas boundary and locate such key “landmarks” as the critical point. Establishing the existence of this critical point would be a seminal step forwards for QCD physics. The BES would also allow us to determine the collision energy at which a sQGP is no longer made, by identifying the $\sqrt{s_{NN}}$ at which the signals associated with the plasma are no longer observed. Finally the BES could be used to further study the potential local parity violation signal discussed above. If it is a parity violation signal the effect should be stronger at lower collision energies, as the time integral of the magnetic field is larger. The signal should however not persist at collision energies where no sQGP signals are formed since the parity violating effect is dependent on de-confinement.

4.2. The Large Hadron Collider

A new energy window for particle physics is set to open at the end of 2009 when the LHC commences operation. First Pb-Pb collisions at $\sqrt{s_{NN}} = 5.5$ TeV are currently scheduled for the end of 2010. This order of magnitude increase in collision energy will allow the realm of jet and heavy flavor physics, just starting to be exploited at RHIC, to be fully explored with high statistics. The initial conditions will be hotter and denser, and the medium produced is predicted to be larger and longer lived than that currently being studied by STAR and PHENIX [45], see table 4.2. It will be very interesting to study if the sQGP created is the same or if other, unexpected properties, emerge. Currently there is only one dedicated heavy-ion experiment, ALICE [46], but both CMS [47] and ATLAS [48] have active heavy-ion groups.

In addition, the RHIC accelerator is currently being upgraded (RHIC-II) for higher luminosity running via

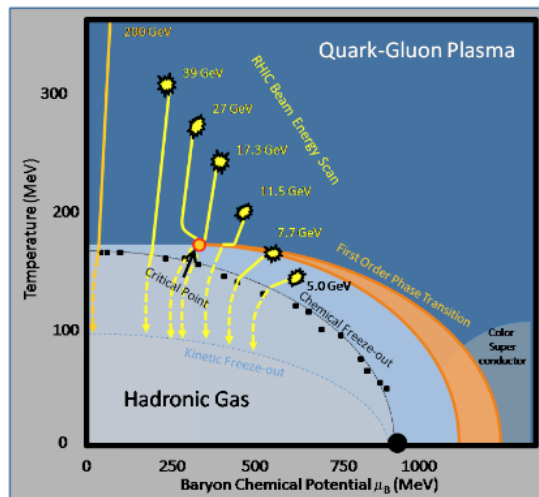


Fig. 11. Color Online: A sketch of the phase diagram of nuclear matter. The location of the critical point is suggestively placed within the RHIC BES range, not estimated from any theoretical calculation. The black closed circles are current heavy-ion experimental calculations of the chemical freeze-out temperature, T_{ch} , and μ_B based on statistical model fits to the measured particle ratios. The yellow curves show the estimated trajectories of the collision energies proposed for the RHIC BES.

stochastic cooling of the beams. While the hard probes studies will certainly be dominated by the LHC results, RHIC will stay competitive in the low to intermediate p_T ranges due to its longer running time per year and higher luminosity after the RHIC-II upgrade. By combining the RHIC and LHC data we will therefore be able to make studies of the physics of heavy-ion phenomena in unprecedented detail from 0.005-5.5 TeV.

Table 1. Comparison of measured RHIC quantities to those expected at the LHC. The physical quantities of the medium are for central Au-Au (RHIC) or Pb-Pb (LHC) collisions at maximum beam energy. The beam measures are for nominal annual heavy-ion running.

	RHIC-II	LHC
Collision energy in A-A	5-200 GeV	5.5 TeV
Initial temperature	$\sim 2T_c$	$\sim 4T_c$
Initial Energy density	5 GeV/fm ³	15-60 GeV/fm ³
Lifetime	2-4 fm/c	> 10 fm/c
Data taking period	12 weeks	4 weeks
Ave. A+A L (cm ⁻¹ s ⁻¹)	5x10 ²⁷	5x10 ²⁶
Integrated L (50% uptime)	20nb ⁻¹	500μb ⁻¹

5. Summary

There are many new and exciting results being produced at RHIC.

While a complete theoretical understanding of these data is still not established, there are many predictions left for heavy-ion experiments to test. Key questions that remain not fully answered are

- How do partons interact with the sQGP and what are the exact mechanisms of their energy loss?
- What are the properties of the medium produced and how they change with differing initial conditions?

- What and where are the key landmarks on the QCD phase diagram of nuclear matter?
- Can the possible signal of local strong parity violation, seen in RHIC collisions and a fundamental prediction of QCD, be explained by any other more mundane signals.

RHIC and the LHC have exciting new programs starting in 2010 which will attempt to answer these, and other questions. The results from the experiments based at these colliders will provide new and complimentary data with which to explore QCD under extreme conditions.

References

- [1] M. Adamczyk *et al.* (BRAHMS Collaboration) Nucl. Instrum. Meth. A 499 (2003) 437.
- [2] K. Adcox *et al.* (PHENIX Collaboration) Nucl. Instrum. Meth. A 499 (2003) 469.
- [3] B.B. Back *et al.* (PHOBOS Collaboration) Nucl. Instrum. Meth. A 499 (2003) 603.
- [4] K.H. Ackermann *et al.* (STAR Collaboration) Nucl. Instrum. Meth. A 499 (2003) 624.
- [5] V.V. Dixit, E. Suhonen Z. Phys. C (1983) 355.
- [6] Z. Fodor, S.D. Katz arXiv:0908.3341 (2009).
- [7] K. Adcox *et al.* (PHENIX Collaboration) Phys. Rev. Lett. 87 (2001) 052301.
- [8] A. Adare *et al.* (PHENIX Collaboration) arXiv:0804.4168 (2008).
- [9] I. Arsene *et al.* (BRAHMS Collaboration) Nucl. Phys. A 757 (2005), Issue 1, 1.
- [10] K. Adcox *et al.* (PHENIX Collaboration) Nucl. Phys. A 757 (2005), Issue 1, 184.
- [11] B.B. Back *et al.* (PHOBOS Collaboration) Nucl. Phys. A 757 (2005) Issue 2, 28.
- [12] J. Adams *et al.* (STAR Collaboration) Nucl. Phys. A 757 (2005) Issue 2, 102.
- [13] J. Adams *et al.* (STAR Collaboration) Phys. Rev. Lett. 91 (2003) 072304.
- [14] S.S. Adler *et al.* (PHENIX Collaboration) Phys. Rev. Lett. 91(2003) 072301; B.B. Back *et al.* (PHOBOS Collaboration) Phys. Lett. B 578 (2004) :297; J. Adams *et al.* (STAR Collaboration) Phys. Rev. Lett. 91 (2003) 172302.
- [15] R. Baier *et al.* Ann. Rev. Nucl. Part. Sci. 50 (2000) 37; M. Gyulassy *et al.*, nucl-th/0302077 (2003).
- [16] A. Adare *et al.* (PHENIX Collaboration) Phys. Rev. Lett. 101 (2008) 232301.
- [17] M. Cacciari and G. Salam, Phys. Lett. B 641 (2006) 57. M. Cacciari, G. Salem and G. Soyez, JHEP 0804 063, (2008). M. Cacciari and G. Salem, Phys. Lett. B 659 (2008) 119.
- [18] M. G. Albrow *et al.* Nucl. Phys. B160 (1979) 1.
- [19] Y-s. Lai and B.A. Cole arXiv:0806.1499 (2008).
- [20] J. Puttschke (for the STAR Collaboration) Eur. Phys. J. C 61 (2009) 629.
- [21] J. Adams *et al.* (STAR Collaboration) Phys. Rev. Lett. 97 (2006) 252001, Y-s. Lai (for the PHENIX Collaboration) arXiv:0907.4725 (2009).
- [22] T. Sjostrand, S. Mrenna, P. Skands JHEP 0605 026 (2006) arXiv:hep-ph/0603175v2.
- [23] R. Field AIP Conf. Proc. 828 (2006) 163.
- [24] H. Caines (STAR Collaboration) arXiv:0910.5203 (2009).
- [25] H. Caines (STAR Collaboration) arXiv:0907.3460 (2009).
- [26] J. Kapitan (STAR Collaboration) arXiv:0909.2951 (2009).
- [27] E. Bruna (STAR Collaboration) arXiv:0907.4788 (2009).
- [28] YS. Lai (PHENIX Collaboration) arXiv:0907.4725 (2009).
- [29] M. Ploskon (STAR Collaboration) arXiv:0908.1799 (2009).
- [30] M. Miller *et al.* Ann. Rev. Nucl. Part. Sci. 57 (2007) 205.
- [31] J. Puttschke (STAR Collaboration) http://www.bnl.gov/rhic_ags/users_meeting/Workshops/6.asp (2009).
- [32] C.S. Wu *et al.* Phys. Rev 105 (1957) 1413.
- [33] D. Kharveev, R.D. Pisarska and M.H.G. Tytgat Phys. Rev. Lett 81 (1998) 512.
- [34] D. Kharveev Phys. Lett B 633 (2006) 260.
- [35] D. Kharveev, L.D. McLerran and H.J. Warringa Nucl. Phys. A 803 (2008) 227.
- [36] K. Fukushima, D. Kharveev and H.J. Warringa Phys. Rev D 78 (2008) 074033.
- [37] A.M. Poskanzer and S.A. Voloshin Phys. Rev. C 70 (2004) 057901.
- [38] S.A. Voloshin Phys. Rev. C 70 (2004) 057901.
- [39] M. Gyulassy and X.-N Wang Com[ut. Phys. Commun. 83 (1994) 397.
- [40] S.A. Bass *et al* Prog. Part. Nucl. Phys 41 (1998) 255.
- [41] R.L. Ray and R.S. Longacre arXiv:nucl-ex:0008009 (2000).
- [42] B. Abelev *et al.* (STAR Collaboration) arXiv:0909.1717 (2009).
- [43] M.A. Stephanov Prog. Theor. Phys. Suppl. 153 (2004) 139.
- [44] B. Abelev *et al.* (STAR Collaboration) arXiv:0909.1739 (2009).
- [45] N. Armesto *et al.* J. Phys. G: Nucl. Part. Phys. 35 (2008) 054001.
- [46] ALICE Collaboration J. Phys. G: Nucl. Part. Phys. 30 and 32 (2006) 1517, 1295.
- [47] D. d'Enterria *et al.* (CMS Collaboration) J. Phys. G: Nucl. Part. Phys. 34 (2007) 2307.
- [48] ATLAS Technical Design Report Vol 1 and 2 (1999) CERN-LHCC-9914, CERN-LHCC-9915.